OPTIMISATION OF THE GREEN SYNTHESIS PROCESS OF COPPER NANOPARTICLES USING LIME (*Citrus aurantifolia*) EXTRACT USING RESPONSE SURFACE METHODOLOGY WITH THE BOX-BEHNKEN MODEL

Nguyen Vi Thien Thao, Nguyen Thi Mai, Tran Do Thanh Thang, Pham Huy Vu, Nguyen Thi Luong, Le Thi Hong Thuy*

Ho Chi Minh City University of Industry and Trade

*Email: *thuylth@huit.edu.vn*

Received: 4 April 2025; Accepted: 5 May 2025

ABSTRACT

This study presents a green synthesis method for copper nanoparticles (CuNPs) using lime extract (LE) as a reducing agent. The optimisation process was conducted through single-factor experiments and response surface methodology (RSM) with a Box-Behnken design, identifying the optimal conditions: temperature of 50.77 °C, pH 7.68, LE/H_2O ratio of 1.45, Cu^{2+}concentration of 3.0 mM, Polyvinyl alcohol (PVA) concentration of 0.6 g/L, and reaction time of 90 minutes. TEM images revealed that the synthesized CuNPs exhibited a uniform cubic morphology. The particle size determined by dynamic light scattering (DLS) was 21.432 nm, while the crystallite size calculated from X-ray diffraction (XRD) was 21.276 nm. XRD analysis confirmed a face-centered cubic (FCC) crystal structure, consistent with the TEM images and the standard copper reference (JCPDS Card No. 04-0836). The difference in particle sizes measured by DLS and XRD arises from their distinct measurement principles: XRD determines crystallite size, while DLS measures hydrodynamic size. With significantly small particle sizes, the synthesized CuNPs exhibit superior physicochemical properties, offering promising applications in electronics, biomedicine, and agriculture.

Keywords: Copper nanoparticles, green synthesis, lime extract, response surface methodology (RSM), Box-Behnken model.

1. INTRODUCTION

Nanotechnology has garnered significant attention in recent decades due to its extensive applications, particularly in metallic nanomaterials. Copper nanoparticles (CuNPs) are notable for their high electrical and thermal conductivity, vigorous catalytic activity, and outstanding antibacterial and antifungal properties. These properties make them promising materials in electronics, biomedicine, and agriculture, including conductive inks, antibacterial coatings, and crop protection agents [1–3]. Copper nanoparticles can be synthesized using physical, chemical, and biological (green) methods, each offering distinct advantages and limitations. Physical methods, including evaporation–condensation, laser ablation, and arc discharge, typically yield high-purity nanoparticles with well-controlled size and morphology. However, these techniques require high energy consumption and sophisticated equipment, making them less economically viable for large-scale production [4–6]. In contrast, chemical synthesis methods, such as metal salt reduction, polyol synthesis, and sol-gel techniques, allow better control over nanoparticle properties [7, 8]. Although effective, these methods often use toxic reducing agents such as sodium borohydride and hydrazine, leading to toxicity and environmental pollution risks due to harmful by-products [9]. Given these limitations, green synthesis has emerged as a more sustainable and environmentally friendly alternative, employing plant extracts, microorganisms, or biomolecules as reducing and stabilizing agents. Recent studies have shown considerable interest in using plant extracts as reducing agents in synthesising CuNPs due to their environmental friendliness and high efficiency. Bioactive compounds in the plant extract, including polyphenols, flavonoids, tannins, alkaloids, and organics acids, play an important role in reducing Cu^{2+} ions into copper nanoparticles and stabilising

them without toxic chemicals [10]. Various plant extracts have been investigated for their potential in the green synthesis of copper nanoparticles (CuNPs). The leaf extract of *Celastrus paniculatus* Willd. has been utilised as both a photocatalytic and antifungal agent in plants [11]. Extracts from garlic (*Allium sativum*), enriched with sulfur-containing compounds such as allicin, have demonstrated not only the ability to facilitate nanoparticle formation but also a significant enhancement in antibacterial efficacy [12]. Similarly, the outer peel of onion (*Allium cepa*), characterised by a high polyphenol content, has enabled the efficient synthesis of CuNPs at ambient temperature [13]. The leaf extract of *Eclipta prostrata*, known for its abundant antioxidant compounds, has been employed to synthesise CuNPs that exhibit notable biological activities, particularly in biomedical applications [14]. Additionally, lemon (*Citrus limon*) fruit extract, rich in citric acid and flavonoids, has served as a potent reducing and stabilising agent during the CuNPs formation process [1]. These findings demonstrate the diversity of plant materials available and highlight the potential of green synthesis in producing copper nanomaterials with desired properties and environmental benefits.

The lime tree (*Citrus aurantifolia*) is native to Southeast Asia and India. It is now widely grown in many parts of the world, mainly in tropical and subtropical climates [15]. Vietnam is among the significant lime-producing countries, with an abundant supply from provinces such as Đong Nai, Tien Giang, Long An, and Nghe An. Lime fruits are rich in bioactive compounds such as citric acid, vitamin C (ascorbic acid), flavonoids (e.g., hesperidin, eriocitrin), and essential oils**.** These compounds are known for their strong antioxidant, reducing, and stabilizing abilities, making lime extract a promising candidate for the green synthesis of CuNPs [16]. Among them, citric acid and flavonoids are considered the key active components responsible for reducing Cu^{2+} ions and stabilizing the formed nanoparticles. Therefore, lime fruit extract not only offers a sustainable resource but also enhances the efficiency and biocompatibility of synthesized nanoparticles.

Although extensive research has been conducted on the green synthesis of CuNPs, optimizing reaction conditions to control particle size and morphology remains challenging. Most previous studies have focused on single-variable experiments, whereas response surface methodology (RSM), particularly the Box-Behnken model, enables multi-variable analysis and synthesis optimization with minimal experiments [17, 18].

Thus, this study aims to optimize the synthesis process of CuNPs using lime (*Citrus aurantifolia*) whole fruit extract through the Box-Behnken model (RSM). Key parameters, including Cu^{2+} concentration, extract ratio, pH, temperature, and reaction time, will be investigated to identify the three most significant factors for optimization. The synthesized CuNPs will be characterized using TEM, XRD, and particle size distribution analysis, providing better control over their properties for potential applications.

2. MATERIALS AND METHODS

2.1 Materials

The chemicals used in this study include copper (II) sulfate pentahydrate ($CuSO_4 \cdot 5H_2O$, 99%, Xilong), sodium hydroxide (NaOH, 98%, Xilong), and polyvinyl alcohol (PVA, 98%, Xilong). All chemicals were used as received without further purification.

The fresh limes (*Citrus aurantifolia*) used in this study were harvested from Thuan Binh, Thach Hoa, Long An. Immediately after harvesting, the limes were transported to the laboratory and processed to obtain the extract on the same day to ensure the preservation of bioactive compounds.

2.2. Preparation of lime extracts (LE)

The extraction of lime was performed based on the methodology reported by Mohammad and Akl, with modifications to suit experimental conditions [1]. Fresh whole limes (including peel, pulp, and juice) were thoroughly washed, cut into small pieces (without separating the peel)**,** and immersed in double-distilled water at a ratio of 1:5 (w/v). The mixture was heated at 80 °C for 10 minutes in a 250 mL glass beaker. After the extraction, the solution was filtered using Whatman No. 41 filter paper to remove solid residues. The clear filtrate was then stored in a sealed glass flask at 4 °C until further use in the synthesis of copper nanoparticles (CuNPs).

2.3. Green synthesis of CuNPs using LE

The synthesis of copper nanoparticles (CuNPs) was carried out based on the method described by Mohammad and Akl, with modifications to optimize reaction conditions[1]. First, 100 mL of prepared LE was mixed with PVA to create a stable dispersion medium. The pH of the solution was then adjusted using 0.1 M NaOH solution. The mixture was heated to the designated temperature, after which a Cu^{2+} solution was gradually added dropwise while stirring continuously. The formation of CuNPs was confirmed by a color change in the solution from blue to brown. After the reaction, the solution was centrifuged at 3000 rpm for 10 minutes to collect the nanoparticles. The obtained CuNPs were then washed with double-distilled water and ethanol to remove residual impurities, followed by drying in an oven at 80–90 °C for 4 hours before structural and property characterization.

The investigated parameters and their respective ranges included reaction temperature (30–70 °C), reaction time (30–150 minutes), PVA concentration (0.4–1.2 g/L), lime extract-to-water (LE/H_2O) volume ratio factor (1–3 times), pH (6–10), and Cu^{2+} concentration (1–5 mM).

2.4. Design of experiment

The RSM was employed to optimize the synthesis of CuNPs using lime extract. Three key factors influencing CuNPs formation, including reaction temperature, lime extract-to-water (LE/H_2O) volume ratio, and pH, were investigated to determine the optimal synthesis conditions. These factors play a crucial role in the green synthesis of CuNPs.

In all experiments, the total volume of the diluted solution was fixed at 100 mL, while other parameters, such as Cu^{2+} concentration, PVA concentration, and reaction time, were kept constant based on preliminary single-factor experiments. The response variable was the maximum absorbance (A_{max}) at the characteristic wavelength (λ_{max}) of CuNPs, measured using UV-Vis spectroscopy. A total of 15 experiments were designed following the Box-Behnken model, with three independent variables examined at three different levels (Table 1). The specific conditions of each experiment are detailed in Table 3.

Table 1. Coded values of independent variables

No.	Independent variable	Code	Experimental levels		
			-1	0	+1
1	Temperature (°C)	x_1	$T_o - 10$	T_o	$T_o + 10$
2	LE/H_2O Ratio (v/v)	x_2	$R_o - 0.5$	R_o	$R_o + 0.5$
3	pH	x_3	$pH_o - 1$	pH_o	$pH_o + 1$

(T_o, R_o, pH_o represent the optimum values of temperature, LE/H_2O ratio, and pH, respectively, determined from the single-factor survey results)

After conducting all 15 experiments and collecting the corresponding response data, the optimal synthesis conditions for CuNPs were determined. Statistical analysis was performed CuNPs using ANOVA in Minitab 16. The most suitable model was selected based on variance analysis results, and a second-order regression equation was established to describe the relationship between independent variables and the response. The regression coefficients were determined through experimental data analysis, enabling the development of a quadratic regression equation following the response surface model [19].

$$Y = \beta_o + \sum_{j=1}^{k} \beta_j x_j + \sum_{i<j} \sum \beta_{ij} x_i x_j + \sum_{j=1}^{k} \beta_{ij} x_j^2 \quad (1)$$

Where Y is the predicted response, β_o is the constant coefficient, β_j is the linear coefficient, β_{ij} is the interaction coefficient, β_{jj} is the pure second-order or quadratic effects, x are the design factors.

2.5. Chemical composition analysis

The physicochemical properties of the lime extract, including moisture content, pH, total ash content, total acid content (expressed as % citric acid), and ascorbic acid content (mg/100 g), were determined using standard methods. Moisture content was measured according to AOAC Official Method 934.06. The pH was determined with a calibrated pH meter, following AOAC Official Method 981.12. Total ash content was analysed using the TCVN 10691:2015 standard (equivalent to EN

1135:1994). Total acid content was determined according to AOAC Official Method 942.15. Ascorbic acid content was quantified following the ISO 6557-2 standard.

2.6. Structural and morphological characterization

UV-Vis spectroscopy

The formation and optical properties of CuNPs were monitored using a UV-Vis spectrophotometer (JASCO V-730, Japan). The absorption spectra were recorded in the wavelength range of 200–800 nm to determine the surface plasmon resonance (SPR) peak of CuNPs, which indicates nanoparticle formation.

Transmission electron microscopy (TEM)

The morphological characteristics, including particle shape and size distribution, were observed using transmission electron microscopy (TEM, FEI Tecnai G2 20 S-TWIN, USA). The sample was prepared by depositing a drop of the CuNP dispersion onto a carbon-coated copper grid, followed by air drying at room temperature before TEM imaging.

Particle size distribution analysis

The hydrodynamic diameter and size distribution of CuNPs were determined using dynamic light scattering (DLS) with an SZ-100 Horiba particle size analyzer (Horiba, Japan). Measurements were performed at room temperature, and the data were analyzed to obtain the size distribution profile.

X-ray diffraction (XRD) analysis

The crystalline structure of CuNPs was characterized using an X-ray diffractometer (SIEMENS Rotan, Germany) with Cu Kα radiation operated at 40 kV and 30 mA. The diffraction patterns were recorded in the 2θ range of 10°–90° to confirm the phase composition and crystallinity of the synthesized CuNPs. The crystallite size of the CuNPs was estimated using the Scherrer equation:

$$D = \frac{K\lambda}{\beta\cos\theta} \quad (2)$$

where D is the crystallite size (nm), K is the Scherrer constant (typically 0.9), λ is the X-ray wavelength (1.5406 Å), β is the full width at half maximum (FWHM) of the most intense diffraction peak (in radians), and θ is the Bragg angle (in radians) [12].

3. RESULTS AND DISCUSSION

3.1. LE composition

The analysis results of lime extract composition (Table 2) show that the physicochemical parameters are consistent with previous studies. Still, some differences exist due to lime variety, cultivation conditions, and extraction methods. The citric acid content is 6.49%, consistent with the report by Książek, contributing to sensory characteristics and industrial applications [20]. Notably, citric acid acts as a dispersing agent, improving the stability of copper nanoparticles by forming stable complexes with metal ions [21]. The ascorbic acid content is 30.03 mg/100g, lower than the study by Herbig and Renard, possibly due to storage conditions or extraction methods [22]. Ascorbic acid is a potent reducing agent that reduces Cu^{2+} ions during the green synthesis of copper nanoparticles [23]. Overall, LE has a high moisture content and is rich in citric and ascorbic acids, making it suitable for nanomaterial synthesis, food, and pharmaceutical applications.

Table 2. Analysis results of LE composition

No.	Analysis criteria	Value
1	Moisture content (%)	85.14 ± 0.17
2	pH	2.15 ± 0.02
3	Total ash content (%)	0.54 ± 0.04
4	Total acid content (% citric acid)	6.49 ± 0.03
5	Ascorbic acid content (mg/100g)	30.03 ± 2.56

3.2. Preliminary investigation of factors affecting the synthesis of CuNPs

3.2.1. Formation of CuNPs

The successful synthesis of copper nanoparticles (CuNPs) is demonstrated in Figure 1. The UV–Vis absorption spectrum (Figure 1A) of the CuNPs containing solution shows two characteristic peaks at 256 nm and 564 nm. The peak at 564 nm is attributed to the surface plasmon resonance (SPR) of metallic copper (Cu^0) nanoparticles, indicating that the reduction process and formation of CuNPs have occurred successfully. This finding is consistent with previous studies, in which SPR peaks of CuNPs are typically observed in the range of 550–580 nm, depending on the size and morphology of the particles [1]. The absorption peak at 256 nm indicates the presence of Cu_2O nanoparticles. This coexistence is considered advantageous for agricultural applications, as both CuNPs and Cu_2O nanoparticles have been shown to exhibit strong antifungal activity. Their combination may enhance the effectiveness in controlling plant pathogenic fungi [1, 23].

Control samples containing only $CuSO_4$, PVA, or lime extract (LE) did not show these characteristic peaks, confirming that the observed spectral features are associated specifically with the formation of CuNPs. In addition, the colour change of the solution from light blue ($CuSO_4$) to dark brown (CuNPs), as shown in Figure 1B, provides further visual evidence of the reduction reaction and successful synthesis of copper nanoparticles.

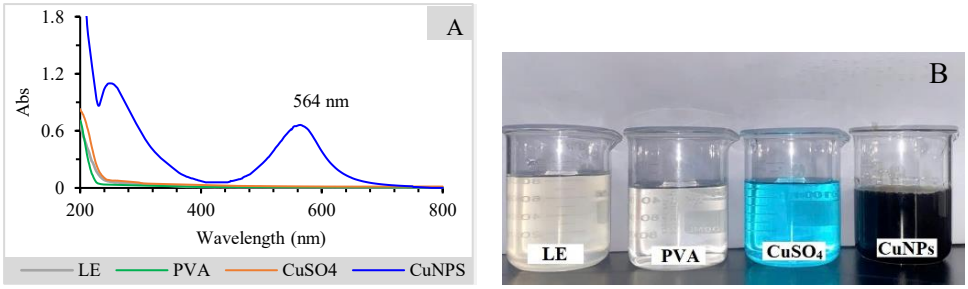

Fig 1. UV–Vis spectrum of LE, PVA, $CuSO_4$, and CuNPs (A). Appearance of the respective solutions (B) *(Cu^{2+}: 3 mM; pH: 8; LE/Cu^{2+}: 2; PVA: 0.8 g/L; Temp: 50 °C; Time: 40 min)*

3.2.2. Influence of reaction parameters on the formation and stability of CuNPs

The synthesis process of copper nanoparticles (CuNPs) using LE as a reducing agent was investigated through a single-factor approach. Factors such as Cu^{2+} concentration, PVA content, pH, temperature, reaction time, and the extract-to-water ratio (LE/H_2O) were evaluated to determine their impact on the formation and stability of CuNPs.

The influence of Cu^{2+} concentration (Figure 2) shows that increasing the precursor concentration from 1 mM to 3 mM enhances SPR intensity, indicating improved nanoparticle formation (Figure 2A). However, at concentrations of 4-5 mM, the absorbance decreases (Figure 2B), likely due to the aggregation of particles caused by an excess of Cu^{2+} ions. A similar trend was reported by Saran et al. (2018), highlighting the effect of high metal ion concentrations on colloidal stability [25]. Consequently, 3 mM Cu^{2+} was identified as the optimal concentration. Figure 3 illustrates that as the pH increases from 6 to 10, the absorbance also rises, reaching a maximum at pH 10 (Figure 3B). However, the broader absorption peaks observed at pH 9 and 10 suggest nanoparticle aggregation and increased polydispersity, which reduce the stability of the CuNPs [19]. In contrast, at pH 8, the surface plasmon resonance (SPR) peak is sharper, indicating the formation of more uniform copper nanoparticles. Therefore, pH 8 was identified as the optimal value for the synthesis process. The effect of PVA concentration is shown in Figure 4, which indicates that increasing the PVA concentration from 0.4 g/L to 0.8 g/L enhances the stability of CuNPs by preventing their aggregation. However, beyond 1.0 g/L, the absorbance reaches a plateau, suggesting that excessive PVA may hinder nanoparticle formation. Figure 5 demonstrates that increasing the LE/H_2O ratio from 1 to 1.5 improves nanoparticle yield. However, further dilution (LE/$H_2O \geq 1.5$) reduces synthesis efficiency, possibly due to an insufficient concentration of reducing agents. The influence of temperature (Figure 6) indicates that CuNPs synthesis is most effective at 50 °C; beyond this point, aggregation occurs, reducing colloidal stability [10]. The effect of reaction time (Figure 7) shows that the formation of CuNPs increases significantly as the reaction time extends to 90 minutes. Beyond this point, the formation continues only slightly,

indicating that the reaction has reached its final stage [10]. Therefore, a reaction time of 90 minutes is considered optimal for synthesising copper nanoparticles.

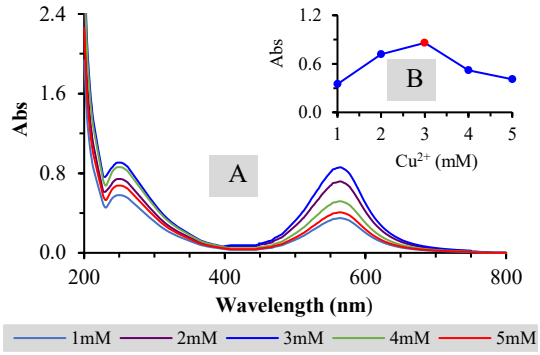

Figure 2. UV-Vis spectra of CuNPs (A) and absorbance at 564 nm under different Cu^{2+} concentrations (B)
(pH: 8; LE/Cu^{2+}: 2; PVA: 0.8 g/L; Temp: 50 °C; Time: 90 min)

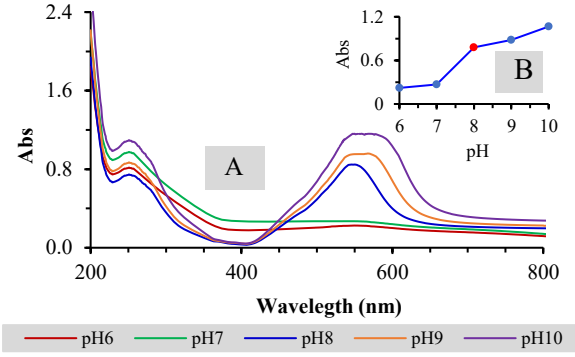

Figure 3. UV.Vis spectra of CuNPs (A) and absorbance at 564 nm under different pH values (B)
(Cu^{2+}: 3 mM; LE/Cu^{2+}: 2; PVA: 0.8 g/L; Temp: 50 °C; Time: 90 min)

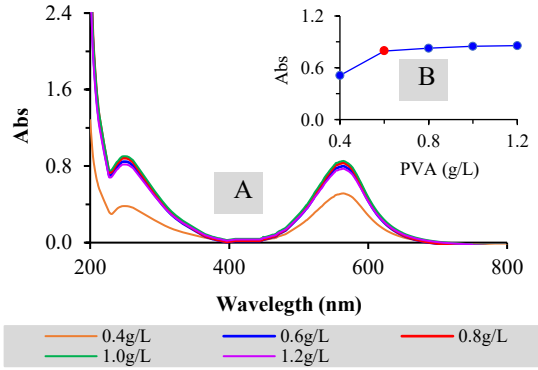

Figure 4. UV-Vis spectra of CuNPs (A) and absorbance at 564 nm under different PVA concentrations (B)
(Cu^{2+}: 3 mM; pH: 8; LE/Cu^{2+}:2; Temp: 50 °C; Time: 90 min)

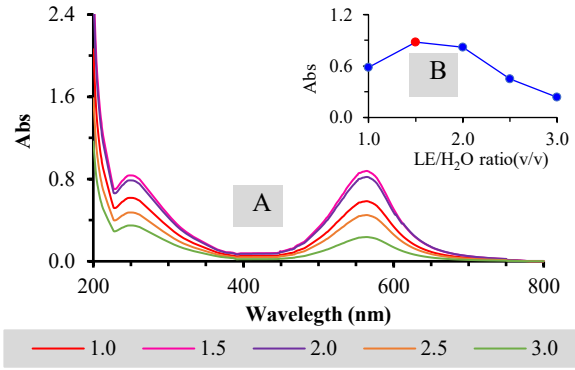

Figure 5. UV–Vis spectra of CuNPs (A) and absorbance at 564 nm under different LE/H_2O ratio (B)
(Cu^{2+}: 3 mM; pH: 8; PVA: 0.6g/L; Temp: 50 °C; Time: 90 min)

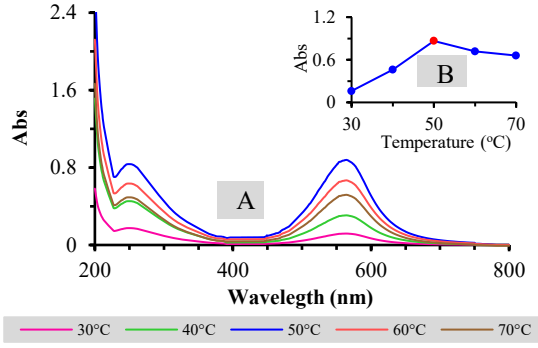

Figure 6. UV–Vis spectra of CuNPs (A) and absorbance at 564 nm under different temperatures (B)
(Cu^{2+}:3 mM; pH: 8; PVA: 0.6g/L; LE/Cu^{2+}:1.5; Time: 90 min)

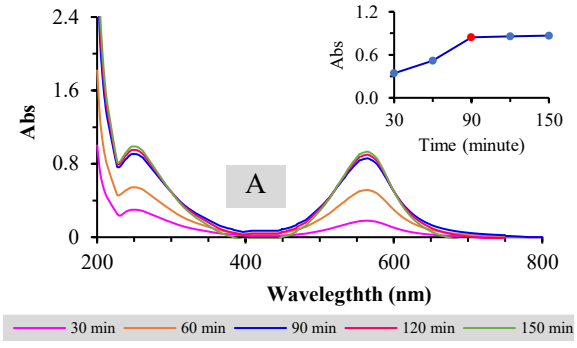

Figure 7. UV–Vis spectra of CuNPs (A) and absorbance at 564 nm over different reaction times (B)
(Cu^{2+}: 3 mM; pH: 8; PVA: 0.6g/L; LE/Cu^{2+}: 2; Temp: 50 °C;)

Based on these investigations, the optimal synthesis conditions were determined to be a Cu^{2+} concentration of 3 mM, pH 8, LE/H_2O ratio of 1.5, PVA concentration of 0.6 g/L, temperature of 50 °C, and a reaction time of 90 minutes. Among these parameters, pH, LE/H_2O ratio, and temperature exhibited the most significant influence and should be further optimized using Response Surface Methodology (RSM) to refine the synthesis process.

3.3. Optimization of CuNPs synthesis using RSM

The response surface methodology (RSM) using the Box-Behnken model was employed to design the experimental matrix, and the absorbance values (Y) from 15 experiments, along with the predicted values (Y') from JMP 17 software, are presented in Table 3. The experimental results indicate that the absorbance values range from 0.474 to 0.908, while the predicted values from the model range from 0.460 to 0.887. The close agreement between these values demonstrates the model's strong predictive capability for CuNPs synthesis efficiency.

Table 3. Experimental values and predicted model results

No.	LE/H_2O ratio		Temperature		pH		Absorbance intensity	
	Coded	Actual (v/v)	Coded	Actual (°C)	Coded	Actual	Experimental values (Y)	Predicted model values (Y')
1	+1	2.0	0	50	+1	9	0.474 ± 0.014	0.460
2	0	1.5	-1	40	+1	9	0.547 ± 0.012	0.559
3	+1	2.0	-1	40	0	8	0.548 ± 0.001	0.549
4	-1	1.0	0	50	+1	9	0.636 ± 0.009	0.627
5	+1	2.0	+1	60	0	8	0.647 ± 0.003	0.650
6	-1	1.0	0	50	-1	7	0.656 ± 0.003	0.669
7	+1	2.0	0	50	-1	7	0.668 ± 0.008	0.676
8	-1	1.0	-1	40	0	8	0.676 ± 0.004	0.672
9	-1	1.0	+1	60	0	8	0.688 ± 0.002	0.686
10	0	1.5	+1	60	+1	9	0.755 ± 0.010	0.765
11	0	1.5	+1	60	-1	7	0.758 ± 0.013	0.745
12	0	1.5	-1	40	-1	7	0.848 ± 0.010	0.838
13	0	1.5	0	50	0	8	0.883 ± 0.021	0.887
14	0	1.5	0	50	0	8	0.871 ± 0.033	0.887
15	0	1.5	0	50	0	8	0.908 ± 0.054	0.887

Table 4 presents the regression results for the CuNPs synthesis model. Based on the p-values, it is evident that the factors X_2 (LE/H_2O ratio), X_3 (pH), X_1X_3 (interaction between temperature and pH), X_2X_3 (interaction between LE/H_2O ratio and pH), X_1^2 (quadratic term of temperature), X_2^2 (quadratic term of LE/H_2O ratio), and X_3^2 (quadratic term of pH) are statistically significant ($p < 0.05$), indicating their considerable impact on the synthesis process. In contrast, the factors X_1X_2 (interaction between temperature and LE/H_2O ratio) have p-values > 0.05, suggesting that it does not significantly affect the model and can be omitted to simplify the equation without compromising model accuracy. Based on the statistically significant regression coefficients, the regression equation describing the relationship between absorbance intensity and the studied factors is expressed as follows:

$$Y = 0.8873 + 0.0286X_1 - 0.0399X_2 - 0.0648X_3 + 0.0745X_1X_3 - 0.0435X_2X_3 - 0.0645\,X_1^2 - 0.1830\,X_2^2 + 0.0958\,X_3^2$$

Table 4. Estimated regression results for the model

Term	Estimated coefficient	Standard error	t-ratio	Probability (p-value)
Constant	0.8873	0.010882	81.54	<.0001*
X_1 (Temperature)	0.0286	0.006664	4.30	0.0077*
X_2 (LE/H_2O ratio)	0.0399	0.006664	-5.98	0.0019*
X_3 (pH)	-0.0648	0.006664	-9.72	0.0002*
X_1X_2	0.0218	0.009417	2.31	0.0691
X_1X_3	0.0745	0.009417	7.91	0.0007*
X_2X_3	-0.0435	0.009417	-4.62	0.0058*
X_1^2	-0.0645	0.009809	-6.58	0.0012*
X_2^2	-0.1830	0.009089	-18.66	<.0001*
X_3^2	0.0958	0.009809	9.77	0.0002*

Table 5 presents the analysis of variance (ANOVA) results for the response surface methodology (RSM) model based on the Box-Behnken design, applied to the green synthesis of copper nanoparticles using lime extract. The Prob > F value of 0.0011 is less than the threshold of 0.05, indicating that the model is statistically significant at a 95% confidence level. The high F-value (26.1557) further confirms that the independent variables have a substantial effect on the response variable, affirming the adequacy of the model. A Prob > F of 0.5366 from the lack of fit test, being well above 0.05, confirms that the model adequately fits the experimental data without significant deviation. This means the model is consistent with the experimental data and does not miss any important trend. The adjusted coefficient of determination $R^2_{adj} = 0.9571$ reveals that 95.71% of the variance in the response is explained by the model, indicating an excellent model fit.

Table 5. Analysis of variance and Lack of fit

Source		DF	Sum of squares	Mean square	F ratio	Prob > F	R
Analysis of variance	Model	9	0.25939998	0.028822	26.1557		R^2_{adj} 0.9571
	Error	5	0.00550975	0.001102			
	C. Total	14	0.26490973			0.0011*	
Lack of fit	Lack of fit	3	0.00106375	0.000355	0.9951	0.5366	Max Rsq 0.9971
	Pure error	2	0.00071267	0.00356			
	Total error	5	0.00177642				

Figure 8 illustrates the optimisation plots for absorbance and desirability, demonstrating the response surface methodology's ability to predict optimal conditions for synthesis. The highest absorbance value (0.897) is observed at an LE/H_2O ratio of approximately 1.45, a temperature of 50.77 °C, and a pH of 7.68, indicating these as the most favourable conditions for maximising synthesis efficiency. Figure 9 presents the regression plot of actual versus predicted absorbance values. The coefficient of determination (R^2) of 0.9926 and a p-value < 0.0001 confirm the model's strong predictive power and statistical significance. The root mean square error (RMSE) of 0.0188 indicates minimal deviation between predicted and experimental values, further validating the reliability of the regression model.

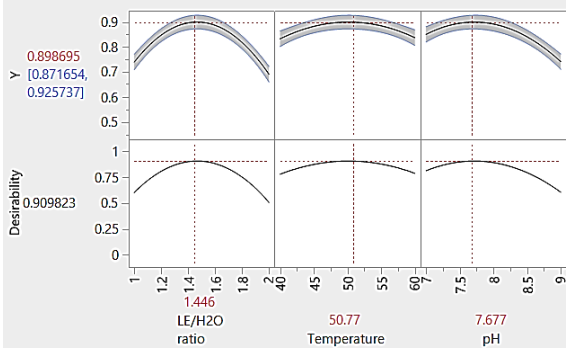

Figure 8. Optimization plot for absorbance and desirability

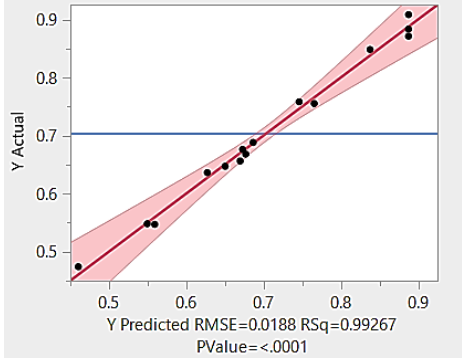

Figure 9. Regression plot of actual vs. predicted absorbance

Figure 10 illustrates the response surface plots depicting the interaction effects of the independent variables on absorbance. The plots indicate significant two-factor interactions - specifically between the LE/H_2O ratio and temperature, LE/H_2O ratio and pH, and pH and temperature - emphasising the nonlinear nature of the system. The LE/H_2O ratio and temperature show a parabolic relationship with absorbance, indicating that an optimal balance is required to achieve maximum efficiency. Similarly, pH significantly influences absorbance, with a decrease at extreme values, emphasising the importance of maintaining a controlled pH range for optimal CuNPs synthesis. These findings collectively support the validity of the model and its applicability in optimising the synthesis conditions.

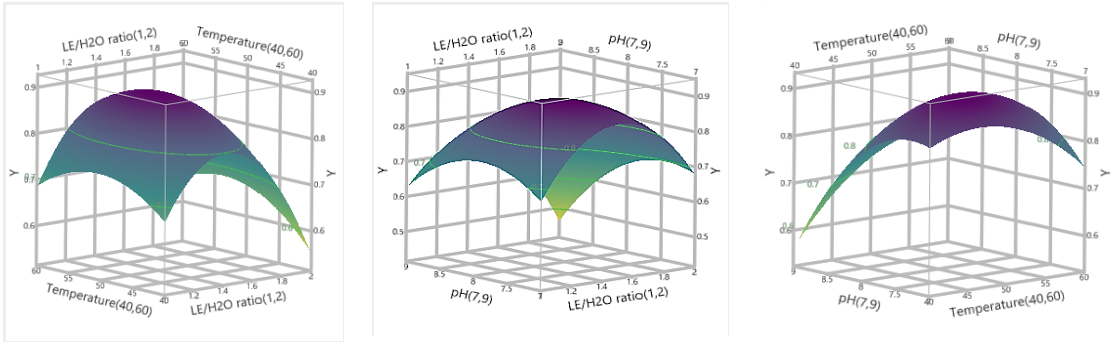

LE/H_2O × Temperature | LE/H_2O × pH | pH × Temperature

Figure 10. Response surface plots for the interaction effects of independent variables on absorbance

After determining the optimal conditions, the model's results were validated through experimental verification. When repeating the experiment three times at the optimal point, the obtained absorbance value was 0.895. The predicted absorbance (0.898) and the experimental results showed no statistically significant difference ($p<0.05$), demonstrating that the optimized model is highly accurate and applicable to the synthesis process of copper nanoparticles using lime extract as a reducing agent. The conditions for copper processing with fixed inputs, including Cu^{2+} concentration of 3 mM, PVA concentration of 0.6 g/L, and a reaction time of 90 minutes, is temperature of 50.77 °C, pH of 7.68, LE/H_2O ratio of 1.45.

3.4. Characterization of copper nanoparticle

The TEM images of CuNPs synthesised under optimal conditions, captured at magnifications of 100,000× (Figure 11), reveal that the nanoparticles exhibit a characteristic cubic shape with slight aggregation. This aggregation may result from electrostatic attraction or particle interactions during synthesis. The particle diameters range from 10 to 30 nm, with some larger particles observed due to aggregation phenomena. The particle size distribution diagram of CuNPs (Figure 12) shows an average particle size (Z-Average) of 21.432 nm with a polydispersity index (PDI) of 0.278. A PDI value below 0.3 indicates a uniform particle size distribution, confirming that the LE synthesis method produces relatively stable nanoparticles. The particle size results for CuNPs in this study align with previously published data, showing stable and uniformly distributed sizes. Amer and Awwad (2024) synthesised CuNPs using citrus limon fruit extract and obtained an average particle size of 28 nm, with more significant aggregation [26]. Similarly, Khurramovna et al. (2024) synthesised CuNPs using peel extracts from various citrus fruits, achieving an average particle size of 22.4 nm with a narrow size distribution and maintaining colloidal stability for over three months [15].

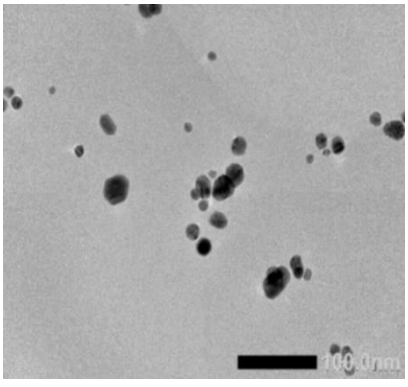

Figure 11. TEM images of CuNPs at 100 000× magnification

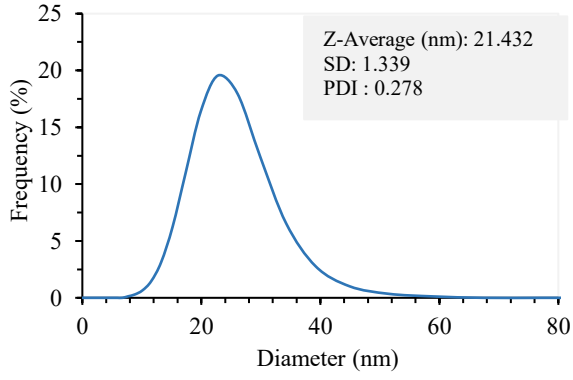

Figure 12. Particle size distribution diagram of CuNPs

The XRD spectrum of CuNPs in Figure 13 exhibits characteristic diffraction peaks at 2θ angles of approximately 43.3°, 50.4°, and 74.1°, corresponding to the (111), (200), and (220) crystal planes of

metallic copper (JCPDS Card No. 04-0836). Additionally, weaker diffraction peaks appear at 36.4° and 61.3°, which belong to Cu_2O (JCPDS No. 05-0667), indicating that a small amount of copper (I) oxide may have formed during the synthesis process. This result confirms that the synthesised CuNPs prossess a face-centred cubic (FCC) crystal structure characteristic of CuNPs, while the minor presence of Cu_2O is likely due to slight surface oxidation. Compared with the TEM images (Figure 11), it is evident that the CuNPs have a cubic morphology and are relatively well-dispersed. The average particle size estimated from XRD using the Scherrer equation is 21.276 nm, which is smaller than the value obtained from the particle size distribution diagram by DLS (21.432 nm). This discrepancy can be explained by the fundamental principles of the two measurement techniques. XRD determines the crystallite size based on the broadening of diffraction peaks, reflecting the dimensions of coherent crystalline domains within the particles. In contrast, DLS measures the hydrodynamic diameter of particles in solution, including the solvent shell and any stabilising agents or coatings on the particle surface, leading to a larger measured size. It is also sensitive to aggregation, potentially inflating the average particle size. Compared to previous studies, these results align with the findings of Sadia et al., where biologically synthesised CuNPs exhibited an FCC structure with an average particle size ranging from 5.55–63.60 nm [27]. Similarly, the study by Raveesha and Pramila reported that green-synthesised CuNPs contained a small amount of Cu_2O, consistent with the XRD spectrum in this study [28].

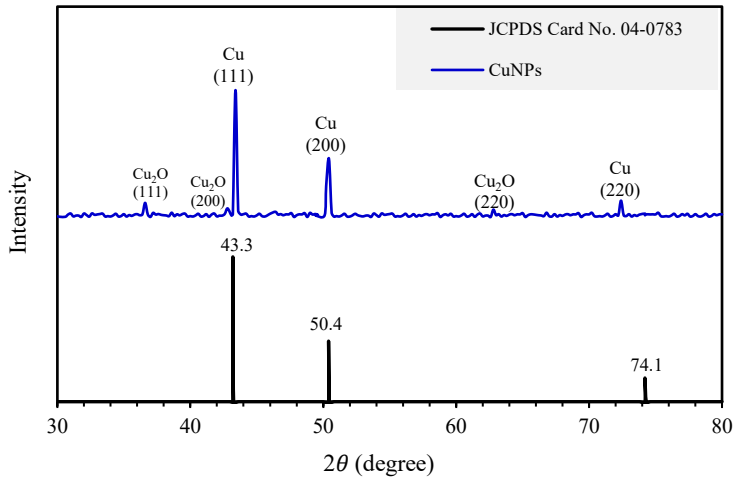

Figure 13. XRD pattern of CuNPs

4. CONCLUSIONS

The study successfully optimized the green synthesis of CuNPs using lime extract. The optimization process was conducted in two stages: single-factor optimization and RSM using a Box-Behnken model to identify key reaction parameters. The optimal conditions were determined as follows: a temperature of 50.77 °C, pH 7.68, an LE/H_2O ratio of 1.45, a Cu^{2+} concentration of 3 mM, a PVA concentration of 0.6 g/L, and a reaction time of 90 minutes. TEM images confirmed that the synthesized CuNPs exhibited a uniform cubic morphology under optimal conditions. DLS analysis measured an average particle size of 21.432 nm with a narrow size distribution, indicating high uniformity. Meanwhile, XRD analysis determined a crystallite size of 21.276 nm and confirmed a face-centered cubic (FCC) crystal structure, consistent with the TEM images and the standard copper reference (JCPDS Card No. 04-0836). The size discrepancy between DLS and XRD measurements arises from their differing measurement principles: XRD determines crystallite size, whereas DLS measures hydrodynamic size. Due to their reduced particle size, the synthesised CuNPs exhibit superior physicochemical properties, offering promising applications in electronics, biomedicine, and agriculture. Overall, this study validates the efficiency and reproducibility of the optimised synthesis process, establishing a strong foundation for further research on large-scale production and practical applications.

Acknowledgments: This work was financially supported by Ho Chi Minh City University of Industry and Trade under Contract No. 166/HD-DCT dated July 15, 2024.

REFERENCES

1. Mohammad W.A., Akl M.A. - Green synthesis of copper nanoparticles by citrus limon fruits extract, characterization and antibacterial activity. Chemistry International **7** (1) (2021) 1-8. https://doi.org/10.5281/zenodo.4017993
2. Tien N.V., My-Sam D.T., Son T.K. - Antifungal activity of gelatin-tapioca starch film and coating containing copper nanoparticles against colletotrichum gloeosporioides causing anthracnose. Journal of Chemistry **2020** (2) (2020) 1-11. https://doi.org/10.1155/2020/6667450
3. Tamilvanan A., Balamurugan K., Ponappa K., Kumar B.M. - Copper nanoparticles: Synthetic strategies, properties and multifunctional application. International Journal Nanoscience **13** (2) (2014) 1430001-22. https://doi.org/10.1142/S0219581X1430006
4. Crisan M.C., Teodora M., Lucian M. - Copper nanoparticles : synthesis and characterization, physiology, toxicity and antimicrobial applications. Applied Sciences **l2** (1) 141 (2022). https://doi.org/10.3390/app12010141
5. Umer A., Naveed S., Ramzan N., Rafique M.S. - Selection of a suitable method for the synthesis of copper nanoparticles. Nano **7** (5) (2012) 1230005-18. https://doi.org/10.1142/S1793292012300058
6. Khanna P.K., Gaikwad S., Adhyapak P.V., Singh N., Marimuthu. - Synthesis and characterization of copper nanoparticles. Materials Letters **61** (25) (2007) 4711-4714. https://doi.org/10.1016/jmatlet.2007.03.014
7. Yadav R.K., Jangeer S., Parashar R., Sharma G., Meena P., Meena M.K., Patel D.D. - A critical review on nanoparticles synthesis : physical, chemical and biological perspectives. International Journal of Creative Research Thoughts **11** (10) (2023) 834-848
8. Salem S.S., Hammad E.N., Mohamed A.A., El-Dougdoug W. - A comprehensive review of nanomaterials: types, synthesis, characterization, and applications. Biointerface Research in Applied Chemistry **13** (1) (2023). https://doi.org/10.33263/BRIAC131.041
9. Dikshir P.K., Kumar J., Amit K.D., Sadhu S., Sharma S., Singh S., Gupta P.K., Kim B.S. - Green synthesis of metallic nanoparticles: applications and limitations. A review. Catalysts **11** (902) (2021) 259-281. https://doi.org/10.1016/B978-0-12-822401-4.00022-2
10. Amjad R., Mubeen B., Ali S.S., Imam S. S., Alshehri S., Ghoneim M.M., Alzarea S. I., Rasool R., Ullah I., Nadeem M. S., Kazmi I. - Green synthesis and characterization of copper nanoparticles using *Fortunella margarita* leaves. Polymers **13** (24) (2021) 4364. https://doi.org/10.3390/polym13244364
11. Mali S. C., Dhaka A., Githala C. K., Trivedi R. - Green synthesis of copper nanoparticles using *Celastrus paniculatus* Willd. leaf extract and their photocatalytic and antifungal properties. Biotechnology Reports **27** (2020) e00518. https://doi.org/10.1016/j.btre.2020. e00518
12. Joseph A.T., Prakash P., Narvi S.S. - Phytofabrication and characterization of copper nanoparticles using *Allium sativum* and its antibacterial activity. International Journal of Science, Engineering and Technology **4** (2) (2016) 463-472
13. Akinniyi J. N. - Synthesis and characterization of copper nanoparticles using *Allium cepa* (L.) outer peel at ambient temperature. Tropical Journal of Natural Product Research **9** (3) (2025), 1144-1149. https://doi.org/10.26538/tjnpr/v9i3.32
14. Chung I.M., Abdul R A., Marimuthu S., Vishnu Kirthi A., Anbarasan K., Padmini P., Rajakumar G. - Green synthesis of copper nanoparticles using *Eclipta prostrata* leaves extract and their antioxidant and cytotoxic activities. Experimental and Therapeutic Medicine **14** (2017) 18-24 https://doi.org/10.3892/etm.2017.4466
15. Khurramovna S.S., Khaydarova D.S., Boltayevich R. A., Murodbekovich A. D., Xasanova N., Durdiev N.K. - Green biosynthesis of copper nanoparticles using citrus fruit extracts for enhanced catalytic and antimicrobial properties. Procedia Environmental Science, Engineering and Management **11** (3) (2024) 347-360

16. Dat H.T., Tuyen K.C., Dung N.T, Huy N.S., Mai V.T. N. - Quality parameters of lime fruits (Citrus sp.) cultivated in Long An province. CTU Journal of Science **57** (2021) 170-176. https://doi.org/10.22144/ctu.jsi.2021.019
17. Khoshnamvand N., Mostafapour F.K., Mohammadi A., Faraji M. - Response surface methodology (RSM) modeling to improve removal of ciprofloxacin from aqueous solutions in photocatalytic process using copper oxide nanoparticles (CuO/UV). AMB Express **8** (1) (2018) 48. https://doi.org/10.1186/s13568-018-0579-2
18. Peng Y., Khaled U., Al-Rashed A.A.A.A., Meer R., Goodarzi M., Sarafraz M.M. - Potential application of Response surface methodology (RSM) for the prediction and optimization of thermal conductivity of aqueous CuO (II) nanofluid: A statistical approach and experimental validation. Physica A: Statistical Mechanics and its Applications **554** (2020) 124353. https://doi.org/10.1016/j.physa.2020.124353
19. Bamise C.T., Oziegbe E.O. - Laboratory analysis of ph and neutralizable acidity of commercial citrus fruits in nigeria department of child dental health, Faculty of Dentistry **7** (2) (2013) 72-76 https://doi.org/10.5829/idosi.abr.2013.7.4.73175
20. Książek E. - Citric Acid: Properties, microbial production, and applications in industries. Molecules **29** (1) (2024) 22. https://doi.org/10.3390/molecules29010022
21. Martí N., Mena P., Cánovas.J.A., Micol V., and Saura D. - Vitamin C and the role of citrus juices as functional food. Nat Prod Commun **4** (5) (2009) 677-700. https://doi.org/10.1177/1934578x0900400506
22. Herbig A.L., Renard C.M.G.C. - Factors that impact the stability of vitamin C at intermediate temperatures in a food matrix. Food Chemistry **220** (2017) 444–51. https://doi.org/10.1016/j.foodchem.2016.10.012
23. Umer A., Naveed S., Ramzan N., Rafique M.S., Imran M. - A green method for the synthesis of copper nanoparticles using L-ascorbic acid. Matéria (Rio de Janeiro) **19** (3) (2014) 197-203. https://doi.org/10.1590/s1517-70762014000300002
24. Asmat-Campos D., Montes de Oca-Vásquez G., Rojas-Jaimes J., Delfín-Narciso D., Juárez-Cortijo L., Nazario-Naveda R., Menezes D. B., Pereira R. and Simbrón de la Cruz M. - Cu_2O nanoparticles synthesized by green and chemical routes, and evaluation of their antibacterial and antifungal effect on functionalized textiles. Biotechnology Reports **37** (2023) e00785. https://doi.org/10.1016/j.btre.2023.e00785
25. Saran M., Vyas S., Mathur M., Bagaria A. - Green synthesis and characterisation of CuNPs: Insights into their potential bioactivity. Journals IET The Institution of Engineering and Techonology **12** (3) (2018) 357–364. https://doi.org/10.1049/iet-nbt.2017.0138
26. Amer M. W. and Awwwad A. - Green synthesis of copper nanoparticles by Citrus limon fruits extract, characterization and antibacterial activity. Chemistry International **7** (1) (2013) 1-8. https://doi.org/ 10.5281/zenodo.4017993
27. Sadia B.O., Cherutoi J.K., Achisa C.M. - Optimization, characterization, and antibacterial activity of copper nanoparticles synthesized using S*enna didymobotrya* root extract, Journal of Nanotechnology (2021) 5611434. https://doi.org/10.1155/2021/5611434
28. Raveesha H.R., Pramila E. - Green synthesis and characterization of Cu and Cu_2O nanoparticles and its biological activities using urginea indica: Pharmaceutical science-nanotechnology. International Journal of Life Science and Pharma Research **12** (4) (2022) 86-97. https://doi.org/10.22376/ijpbs/lpr.2022.12.4.P86-97

TÓM TẮT

TỐI ƯU HÓA QUY TRÌNH TỔNG HỢP NANO ĐỒNG TRONG DỊCH CHIẾT QUẢ CHANH (*Citrus aurantifolia*) BẰNG PHƯƠNG PHÁP BỀ MẶT ĐÁP ỨNG VỚI MÔ HÌNH BOX-BEHNKEN

Nguyễn Vi Thiện Thảo, Nguyễn Thị Mai, Trần Đỗ Thanh Thắng,
Phạm Huy Vũ, Nguyễn Thị Lương, Lê Thị Hồng Thúy*
Trường Đại học Công Thương Thành phố Hồ Chí Minh
*Email: *thuylth@huit.edu.vn*

Nghiên cứu này trình bày phương pháp tổng hợp xanh nano đồng (CuNPs) sử dụng dịch chiết quả chanh (LE) làm tác nhân khử. Quá trình tối ưu hóa được thực hiện thông qua khảo sát đơn yếu tố và phương pháp bề mặt đáp ứng (RSM) với mô hình Box-Behnken, các điều kiện tối ưu gồm: nhiệt độ 50,77 °C, pH 7,68, tỷ lệ LE/H_2O 1,45 (v/v), nồng độ Cu^{2+} 3,0 mM, nồng độ PVA 0,6 g/L và thời gian phản ứng 90 phút. Hình ảnh TEM cho thấy các hạt CuNPs có hình thái lập phương đồng nhất. Kích thước hạt xác định bằng phương pháp tán xạ ánh sáng động (DLS) là 21,432 nm, trong khi kích thước tinh thể từ nhiễu xạ tia X (XRD) là 21,276 nm. Phân tích XRD xác nhận cấu trúc tinh thể lập phương tâm diện (FCC), phù hợp với hình ảnh TEM và mẫu đồng tiêu chuẩn (JCPDS Card No. 04-0836). Sự khác biệt giữa kích thước đo bằng DLS và XRD là do XRD xác định kích thước tinh thể còn DLS đo kích thước hydrodynamic. Với kích thước siêu nhỏ, các hạt CuNPs mang lại tính chất vật lý - hóa học vượt trội, mở ra nhiều ứng dụng tiềm năng trong điện tử, y sinh và nông nghiệp.

Keywords: Hạt nano đồng, tổng hợp xanh, dịch chiết quả chanh, phương pháp bề mặt đáp ứng (RSM), mô hình Box-Behnken.